Hyperautofluorescent Ring Pattern in Retinitis Pigmentosa: Clinical Implications and Modifications Over Time

Alessio Antropoli, Alessandro Arrigo, Lorenzo Bianco, Elena Cavallari, Francesco Bandello, and Maurizio Battaglia Parodi

Department of Ophthalmology, Vita-Salute San Raffaele University, IRCCS San Raffaele Scientific Institute, Milan, Italy

Correspondence: Alessandro Arrigo, IRCCS San Raffaele Scientific Institute, Department of Ophthalmology, Via Olgettina, 60, Milan, Lombardy 20132, Italy; arrigo.alessandro@hsr.it.

Received: February 21, 2023
Accepted: June 29, 2023
Published: September 5, 2023

Citation: Antropoli A, Arrigo A, Bianco L, Cavallari E, Bandello F, Battaglia Parodi M. Hyperautofluorescent ring pattern in retinitis pigmentosa: Clinical implications and modifications over time. *Invest Ophthalmol Vis Sci.* 2023;64(12):8. https://doi.org/10.1167/iovs.64.12.8

Purpose. The purpose of this study was to investigate the relation among hyperautofluorescent ring patterns, visual acuity (VA), and optical coherence tomography (OCT) features in patients with retinitis pigmentosa (RP), and to describe its modifications over time.

Methods. This was a retrospective, longitudinal, and observational study. Clinical and imaging data from the first and last available visits of patients with a clinical diagnosis of RP were reviewed. The ellipsoid zone (EZ) width was measured on OCT acquisitions. Short-wavelength autofluorescence (SW-AF) images were classified based on the hyperautofluorescent ring pattern as absent, regular, and irregular, and their modifications over the follow-up were described. The VA, EZ width, and progression rate were compared among the three groups.

Results. One hundred eight eyes from 54 subjects were included in the study. The hyperautofluorescent ring was not present in 28 eyes (25.9%), appeared regular in 45 eyes (41.7%), and had an irregular pattern in 35 eyes (32.4%). The three groups differed in terms of age, VA, and EZ width (all $P < 0.05$). Additionally, the absence of a hyperautofluorescent ring indicated a faster rate of progression ($P < 0.001$). Throughout the follow-up period, 17 eyes (15.7%) experienced a change in the AF pattern, with irregular rings being more commonly affected.

Conclusions. The hyperautofluorescent ring is a useful tool to frame patients based on their EZ width and VA. We described its possible modifications over time, the knowledge of which can aid clinicians in the interpretation of imaging finding changes of their patients.

Keywords: inherited retinal disease, retinitis pigmentosa (RP), fundus autofluorescence (FAF), optical coherence tomography (OCT), hyperautofluorescent (hyperAF) ring

The term "retinitis pigmentosa" (RP) identifies a heterogeneous group of rod-cone dystrophies characterized by a progressive constriction of the visual field, together with nyctalopia and vision loss, due to the degeneration of both rod- and cone-photoreceptors.[1] Fundus autofluorescence (FAF) is a useful imaging modality for monitoring disease progression in RP, as it highlights the reduction or accumulation of lipofuscin-derived signal as areas of hypo- or hyperautofluorescence.[2] With this technique, a relatively high percentage of patients with RP exhibit a hyperautofluorescent (hyperAF) ring encircling the macular region.[3,4] Previous studies have broadened our knowledge on this FAF response, proving that its perimeter demarcates the transition zone between the healthy and unhealthy retina.[5,6] In more detail, the inner border of the ring corresponds to the area where the ellipsoid zone (EZ) fades, whereas the area outside the ring is characterized by a loss of both the EZ and the external limiting membrane (ELM), leaving the outer nuclear layer directly lying upon the retinal pigmented epithelium (RPE).[7,8] Consequently, both structure and function are relatively well-preserved inside the hyperAF ring, whereas significant outer retinal thinning together with retinal sensitivity loss can be found outside its borders.[6,9–11] The precise mechanism underlying the formation of the hyperAF ring remains uncertain. It is unclear whether it is linked to a metabolism dysfunction resulting in lipofuscin accumulation in the RPE, or if it is caused by the interruption of the inhibitory effect of rhodopsin present in the degenerated outer segment on signal attenuation.[4,9] Nonetheless, many authors investigated its potential as a biomarker for disease progression in RP, and found that its constriction correlated with several clinical and functional parameters, such as visual field and full-field electroretinogram.[5,7,9,10]

On the contrary, the clinical implications and temporal evolution of the hyperAF ring morphology have received limited research attention.[12] This study aims to investigate the relation among hyperAF ring patterns, visual acuity (VA), and optical coherence tomography (OCT) features in patients with RP, as well as to describe their modifications over time.

Methods

This was a retrospective, longitudinal, observational study. We identified patients with a clinical diagnosis of RP by reviewing our prospectively maintained institutional database of inherited retinal diseases (IRDs) followed at the Heredodystrophy Unit of the Department of Ophthalmology of IRCCS San Raffaele Scientific Institute, Milan, Italy. All study procedures were approved by the local institutional review board (protocol multimodal imaging in retinal diseases [MIRD]) and were conducted in adherence with the tenets of the Declaration of Helsinki. Clinical and imaging data between November 2011 and June 2021 from the first and last available follow-up visits were collected. Only eyes having both OCT and FAF acquisitions with a minimum follow-up of 1 year were included. Patients were excluded if they had poor quality images due to any cause (including extensive vitreous floaters and high media opacity) and if they already presented RPE atrophy in the macular region at baseline. We categorized images as "poor quality" if they could not be assigned to a short-wavelength autofluorescence (SW-AF) pattern or if the EZ status could not be assessed on OCT scans. Patients with sector RP were not considered eligible for our study. Each patient's records regarding inheritance mode was reviewed, and the inheritance pattern was categorized as autosomal recessive (AR), autosomal dominant (AD), or X-linked (XL) based on causative alleles. Cases were labeled "unsolved" if identified mutations did not account for the phenotype or if no mutations were found.

Acquisition Protocol

To be included, all patients required a minimum acquisition protocol, including an OCT with the radial pattern of 3 B-scans with a 30-degree angle and a high number of frames (ART > 25) and an SW-AF (488 nm excitation) acquired with a Spectralis HRA + OCT (Heidelberg Engineering, Heidelberg, Germany). The SW-AF images were captured with a field of view of either 55 or 30 degrees such that the whole hyperAF ring could be seen in the image. Additional images, such as near infrared (NIR)-AF images or OCT scans with different patterns, aided the graders' judgments, when available.

Image Analysis

Each SW-AF image was analyzed by two independent graders (authors A.A. and E.C.) and a third senior grader (author M.B.P.) was consulted in case of discrepancy. The hyperAF rings were grouped into three categories based on presence and morphology, using a previously described classification: (1) absent, (2) regular, and (3) irregular.[12] In more detail, eyes were assigned to the (1) absent group whenever an hyperAF ring was deemed as not visible at all; (2) regular rings displayed an elliptic/round shape and clearly distinguishable inner and outer borders; (3) irregular rings included open rings, closed rings with non-elliptic shapes, and any ring without clearly visible margins. Each SW-AF was graded both at baseline and at last follow-up examinations, and changes of the FAF pattern were recorded.

On OCT images, the boundaries of the EZ were identified, and the distance between these two locations was defined as the EZ width.[13] For this purpose, we used the default logarithmic display OCT scans provided by the HEYEX software, which enhance the perception of contrast, thus allowing a correct identification of the EZ boundaries even in eyes with steep posterior macular curvature.[14,15] Measurements were obtained on the horizontal and vertical scans, both at baseline and last follow-up visits, and their average was used for our analyses, including yearly progression rate calculation. The latter was determined by calculating the difference between the baseline EZ width and the final EZ width, divided by the length of the follow-up period. Values ranged from the total scan length (EZ width exceeded the total length of the OCT scan) to a minimum value of 0 µm (EZ not distinguishable).

Statistical Analysis

Analyses were performed using SPSS Statistics 23 (IBM, Armonk, NY, USA). All descriptive data were expressed as mean ± standard deviation (SD) for continuous variables and as frequency and percentages for categorical ones. Testing for normality of continuous variables was assessed using the Kolmogorov-Smirnov test. Frequencies among groups were compared with the Chi-square test. Inter-eye correlations were accounted for using a generalized linear mixed-effect regression model (GLMM) to compare the three FAF patterns. Best corrected visual acuity (BCVA), EZ width, and age were set as dependent variables, whereas the SW-AF pattern variable served as the independent variable. The "subject" variable was included as a random effect. Additionally, the progression rate among the three groups was compared with a multivariate GLMM. The progression rate was the dependent variable, with the SW-AF pattern as the fixed factor, and age and EZ width at baseline as covariates. Again, subjects were treated as random effect. To prevent the "floor effect," eyes were excluded from the analysis if they had an EZ width exceeding the total scan length or if the EZ was indistinguishable (0 µm). A further subdivision of the "absent ring" group based on EZ width was also utilized to report BCVA values.

A logistic regression via generalized estimated equation (GEE) was conducted to determine predictor variables for an FAF pattern switch. The dichotomic variable "pattern switch" was the dependent variable, whereas baseline age, baseline EZ width, and follow-up length were the predictor variables. Correlations between quantitative variables were assessed with the Spearman's test. Cohen's Kappa statistic was calculated separately for the left and right eyes, and the average was used to derive the inter-rater reliability. All tests were 2-sided, and the level of significance was set at $P < 0.05$.

Results

Seventy-six patients were considered for the study. Eighteen patients were excluded because they lacked either a follow-up examination fulfilling the inclusion criteria, or they were only visited once. One patient had RPE atrophy in the macular region, and three patients had poor quality images due to media opacities. Therefore, 108 eyes from 54 subjects were included in the study. Twenty-seven (50%) subjects were women. Mean age was 34.1 ± 13.6 years (range = 6.4–57.7 years) and mean follow-up length was 49.6 ± 24.7 months.

At baseline, the hyperAF ring was not present in 28 eyes (25.9%), appeared regular in 45 eyes (41.7%), and had an irregular pattern in 35 eyes (32.4%). The agreement between

Table 1. Comparisons of Baseline Values Between Different hyperAF Ring Patterns

	Mean ± SD (95% CI)				Pairwise Comparisons[†]		
	Absent	Regular	Irregular	*P* Value[*]	*P (A-R)*	*P (A-I)*	*P (R-I)*
BCVA (logMAR)	0.28 ± 0.05 (0.19–0.37)	0.14 ± 0.03 (0.07–0.21)	0.14 ± 0.04 (0.06–0.21)	**0.025**	**0.013**	**0.017**	0.990
Age, y	38.7 ± 2.5 (33.8–43.6)	35.5 ± 1.9 (31.6–39.3)	28.5 ± 2.2 (24.2–32.9)	**0.007**	0.303	**0.003**	**0.020**
EZ width BL (µm)	3664 ± 425 (2822–4507)	2327 ± 335 (1662–2991)	4565 ± 380 (3812–5319)	**<0.001**	**0.015**	0.117	**< 0.001**
Progression rate (µm/y)[a]	218.2 ± 40.0 (151.8–313.6)	107.0 ± 13.9 (82.6–138.6)	115.7 ± 22.0 (79.3–168.8)	**<0.001**	**0.01**	**0.025**	0.743

[*] *P* values for the generalized linear mixed model effect regression among the three groups.
[†] *P* values for pairwise comparisons only shown when overall *P* is < 0.01.
[a] Age and EZ width as covariates. The "subject" variable is treated as random effect.
BCVA = best corrected visual acuity; AF = autofluorescent; SD = standard deviation; A = absent; R = regular; I = irregular; EZ = ellipsoid zone; BL = baseline.

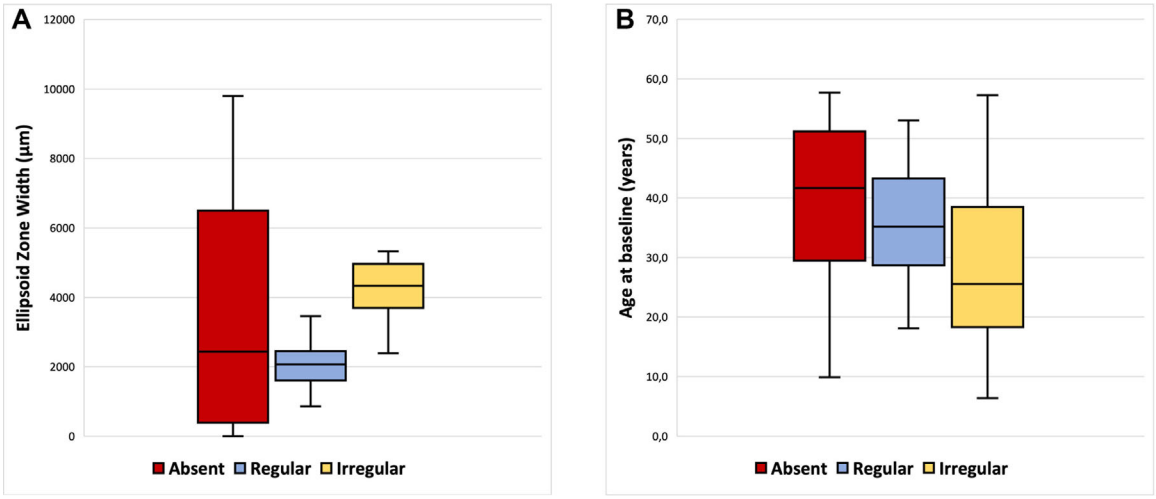

Figure 1. Ellipsoid zone (EZ) width and age comparison between the three groups. (**A**) EZ is shorter in the regular group and wider in the regular group, whereas the absent group has a broader distribution of the EZ width values. (**B**) Eyes from the irregular group belong to the youngest patients, followed by the regular ring group.

the 2 graders was substantial, with an average Kappa value of 0.75 ($P < 0.001$ for both eyes).

On univariate regression with the GLMM, there were statistically significant differences in BCVA, EZ width, and age among the three groups (Table 1). Mean BCVA in the absent, regular, and irregular group were 0.28 ± 0.05, 0.14 ± 0.03, and 0.14 ± 0.04 logMAR (approximately corresponding to 20/40, 20/25, and 20/25 Snellen), respectively ($P = 0.025$). Eyes with irregular rings belonged to the youngest patients, whereas mean age was similar between the absent and regular groups ($P = 0.007$). Given the strong positive correlation between horizontal and vertical EZ measurements (R = 0.965, $P < 0.001$), the following analyses refer to the average of these two values. The raw data pertaining horizontal and vertical EZ width and progression rate can be found in Supplementary Table S1.

Regular rings had the shortest EZ, whereas irregular ones displayed the widest ($P < 0.001$). Conversely, EZ width in eyes without the hyperAF ring had higher variability as testified by the wider interquartile range (IQR) values than the other two groups (Fig. 1). Specifically, median EZ width was 2433 (IQR = 390–6502) µm in the absent ring group, 2076 (IQR = 1605–2456) µm for regular rings, and 4338 (IQR = 3695–4963) µm for the irregular group. Consequently, correlations between EZ width and age, as well as between EZ width and VA were only found in eyes that lacked the hyperAF ring (R = −0.573, $P = 0.001$ and R = −0.682, $P < 0.001$). In addition, in the absent ring group, the EZ on OCT scans can either be intact (>9800 µm), absent (0 µm), or partially preserved (any value in between; Fig. 2). We found that the EZ was intact in 5 out of 28 eyes, partially preserved in 19 cases, and absent in 4 eyes. In this regard, mean BCVA were 0.1 ± 0.1, 0.3 ± 0.1, and 0.5 ± 0.1, in the first, second, and third group, respectively (Fig. 3).

Progression rate for each group was estimated with GLMM after excluding 12 eyes: 9 eyes (4 with absent EZ, 5 with preserved EZ) from the absent ring group, and 3 eyes with an EZ exceeding the scan length from the irregular ring group. In the end, 96 eyes were included in the model, and estimated progression rates, accounting for baseline EZ width and age were calculated. Eyes without a hyperAF ring progressed approximately 88% faster ($P = 0.017$) than those with an irregular ring, which were, in turn, approximatively 7.5% faster ($P = 0.74$) than regular ones, although not statistically significant. In detail, the estimated progression rate of eyes without a hyperAF ring was 218.2 ± 40.0 (confidence interval [CI] = 151.8–313.6) µm/year, significantly faster than both irregular 115.7 ± 22.0 (79.3–168.8) µm/year; pairwise $P = 0.025$, and regular 107.0 ± 13.9 (82.6–138.6) µm/year; pairwise $P = 0.01$ ring eyes (see Table 1). The effect of age was nonsignificant, whereas baseline EZ width had a significant but negligible impact on the progression rate (Table 2).

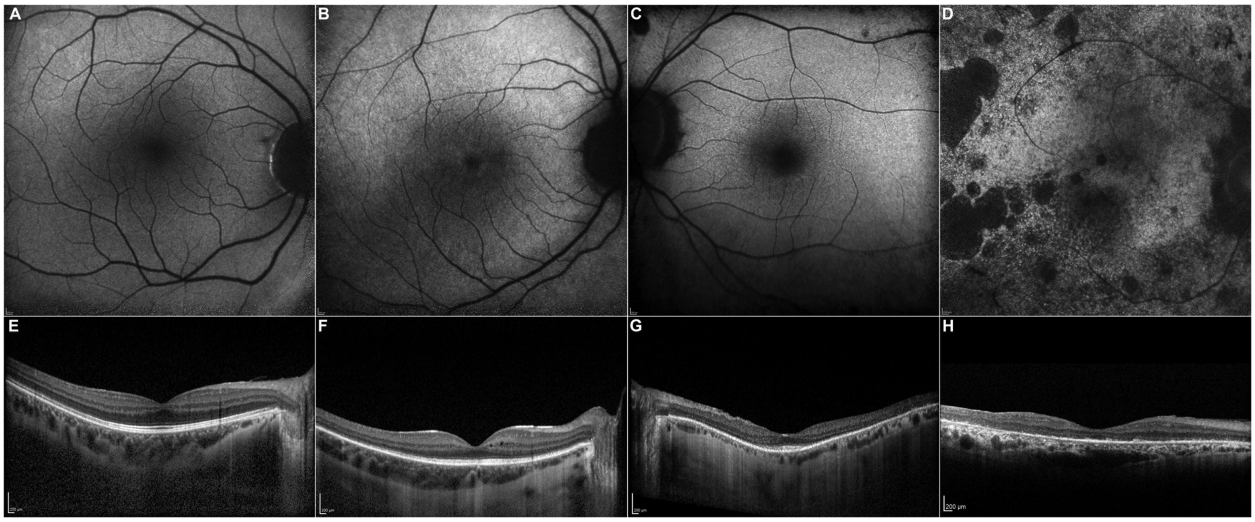

Figure 2. Different ellipsoid zone (EZ) width in eyes without a hyper-autofluorescent (AF) ring. Intact EZ (**A, E**); partially preserved EZ of 7041 µm (**B, F**), and 1816 µm (**C, G**); unmeasurable EZ (**D, H**).

Table 2. Generalized Linear Mixed Model For OCT Progression Rate

	Coefficient	95% CI (Lower Limit–Upper Limit)	*P* Value*
Age, y†	−0.12	−0.026–0.003	0.109
EZ width†	0.00023	0.00012–0.00035	**<0.001**
Absent ring	0.634	0.117–1,151	**0.017**
Regular ring	−0.78	−0.545–0.388	0.740
Irregular ring	*Ref.*	–	–

Dependent variable: Progression rate (µm/year). Coefficients expressed on a logarithmic scale; values converted to original scale represent multiplicative effects associated with each variable on progression rate.

* Statistically significant values in bold.

† Values taken at baseline.

OCT = Optical coherence tomography; CI = confidence interval; EZ = ellipsoid zone.

Last, for 5 out of 54 patients, no causative allele could be found, whereas the remaining 49 cases were distributed as follows: 37 (65.5%) were AR, 8 (14.8%) were AD, and 4 (7.4%) had an XL transmission. Among the recessive RP forms, there were 13 syndromic patients: 3 Usher type 1b, 8 Usher type 2a, and one patient with Bardet-Biedl syndrome. Overall, at baseline, each SW-AF pattern was equally represented among AR RP cases, whereas regular rings were the most common pattern in AD RP eyes, in opposition to XL cases that only displayed irregular or absent ring ($P < 0.001$; Supplementary Table S2).

HyperAF Ring Pattern Modifications Over the Follow-Up

Seventeen (15.7%) out of 108 eyes underwent a pattern switch. Among the 91 eyes maintaining their pattern at the last visit, 26 (28.5%) did not have an hyperAF ring, 42 (46.2%)

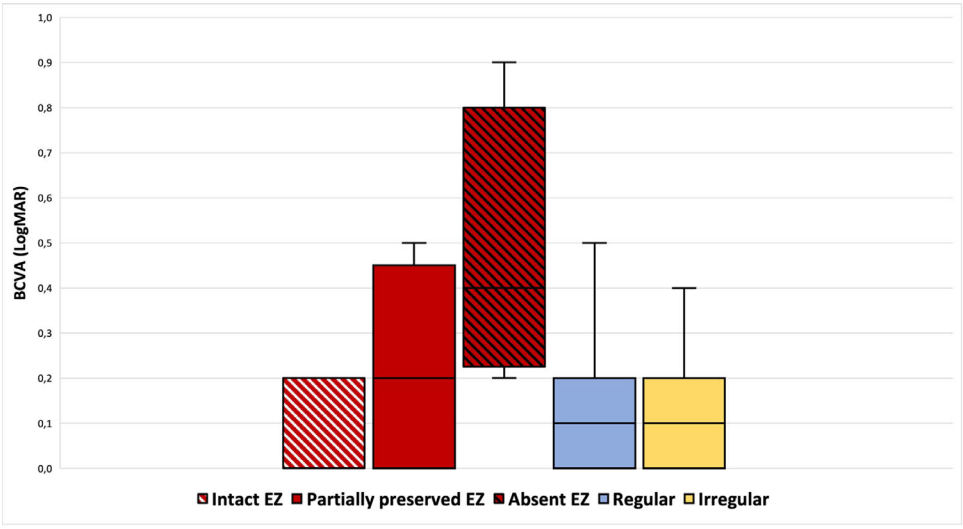

Figure 3. Best-corrected visual acuity (BCVA) comparison between the different SW-AF pattern.

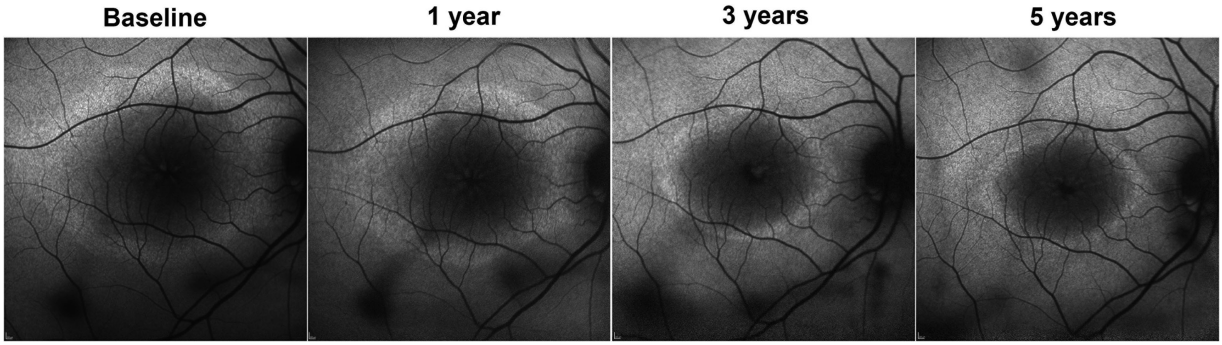

FIGURE 4. Progressive pattern switch from irregular to regular over a 5-year follow-up.

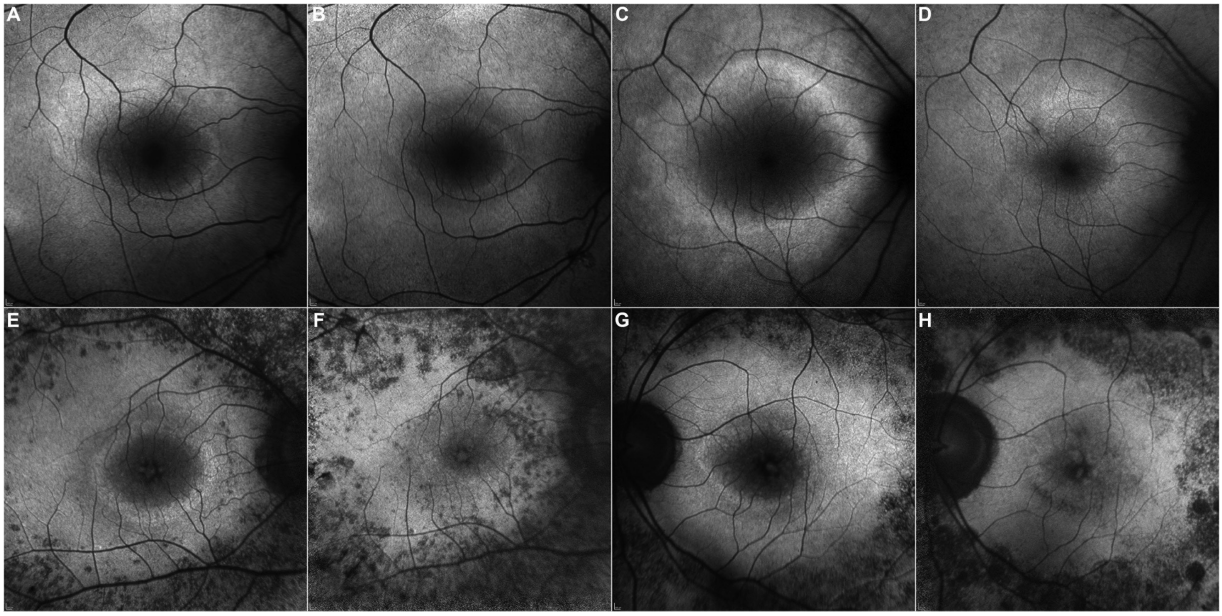

FIGURE 5. **Representative images of different hyperautofluorescent ring pattern switches.** Short wavelength fundus autofluorescence (SW-AF) of 22-year-old patient with an irregular ring (**A**) undergoing a regularization (**B**) over a 2 and one-half year follow-up. (**C**) Irregular ring in a 6-year-old male patient fading away (**D**) over a 6-year follow-up. Switch from regular (**E**) to absent (**F**) ring in a 38-year-old patient over 4 years. Disappearance of the regular ring of a 38-year-old patient over a follow-up of 3 years (**G, H**).

had a regular ring, and 23 (25.3%) had an irregular ring ($P = 0.001$).

On the contrary, 2 (7.1%) eyes from the absent group, 3 (6.7%) eyes from the regular group, and 12 (34.3%) irregular eyes underwent a pattern switch ($P = 0.001$; Figs. 4, 5), without any statistically significant difference between sexes ($P = 0.792$). Finally, at the end of the follow-up, there were 32 (29.6%) absent, 50 (46.3%) regular, and 26 (24.1%) irregular hyper-AF rings (Table 3). Detailed characteristics of the patients that underwent a pattern switch are resumed in Supplementary Table S3. On a logistic regression, age at baseline was the factor associated with a change in the SW-AF pattern over the course of the follow-up ($P = 0.009$), with decreasing odds of undergoing a pattern switch when the age increases, whereas follow-up length and EZ width at baseline were not (Supplementary Table S4).

DISCUSSION

The first classification of RP on SW-AF images was proposed by Murakami et al. in 2008, distinguishing among eyes with a hyperAF ring, eyes with abnormal central AF, and

TABLE 3. Hyperautofluorescent Ring Pattern Modifications Over Time

Total Eyes ($N = 108$)	**Absent**		**Regular**		**Irregular**	
Baseline (%)	28 (25.9)		45 (41.7)		35 (32.4)	
Follow-up (%)	32 (29.6)		50 (46.3)		26 (24.1)	
Pattern change from baseline (%)	2 (7.1)		3 (6.7)		12 (34.3)	
Type of change	**A → R**	**A → I**	**R → A**	**R → I**	**I → A**	**I → R**
	0	2	2	1	4	8

A = absent; R = regular; I = irregular.

eyes lacking both characteristics.[4] The SW-AF pattern could provide information on EZ width, BCVA, and visual field with their system, and they hypothesized that a progression from one pattern to another could exist. Later on, Jauregui et al. proposed a classification that also took account of the hyperAF ring morphology, by dividing them into regular (closed, oval, and defined borders) and irregular (open, closed, with irregular or non-elliptic borders) rings.[12] Our goal was to analyze VA and OCT values of patients with different SW-AF patterns, according to Jauregui et al., and to identify the modifications of the hyperAF ring over time.

According to our findings, the hyperAF ring is a useful tool to frame patients based on their EZ width on OCT and VA. Indeed, both irregular and regular rings showed a quantifiable EZ on OCT images (with the former being larger) and retained a good visual acuity, regardless of their age. However, when the hyperAF ring was missing, both values were quite heterogeneous, necessitating a further subdivision on the basis of OCT findings. Eyes missing a hyperAF ring retained a good BCVA when the EZ was intact, a slightly worse BCVA in case of a measurable EZ, and the worst BCVA when also the EZ was undetectable. Noteworthy, we did not account for the presence of cystoid macular edema, although its presence does not necessarily impair visual acuity in patients with RP.[16]

The correlation between VA and the status of the EZ is already a well-known finding in patients with RP,[17,18] nonetheless, our results suggest that when the hyperAF ring is present, regardless of its dimensions, the EZ is still measurable and predictably VA is still preserved, whereas in its absence defining EZ width still plays a pivotal role in the evaluation of disease stage and progression.[19,20]

Relating to this, several studies found that the rate of progression in RP decreases over time, implying that a faster deterioration occurs earlier in the course of the disease.[21–23] Our results align with these observations because disease progression was slightly faster in the irregular group, composed by younger patients than the regular group. However, the progression rate was considerably higher in the group without a hyperAF ring, irrespective of the patient's age and with minimal influence of the initial EZ width. This finding implies that the absence of a hyperAF ring may indicate a more aggressive disease, whereas its presence is associated with relatively stable disease progression.

Moving to the genetics of our patients, our cohort was mostly composed by patients with RP with an autosomal recessive mode of inheritance, who also demonstrated the highest percentage of irregular rings, whereas AD RP eyes displayed predominantly regular rings, and XL RP eyes fell either in the irregular or absent group. Our results differ from the findings from Jauregui et al., who reported that patients with irregular rings were more likely to be affected by AD RP, probably due to the patients' samples.[12] However, from our perspective, it is more likely that also EZ width, which is related to the inheritance mode, is key in determining the shape of the hyperAF ring.

To the best of our knowledge, this is the first study that focused on the modifications of the shape of the hyperAF ring on SW-AF over time. We observed a pattern switch on SW-AF in roughly 15% of the cases over a mean follow-up of 4 years, with rising odds in younger patients. In our cohort, irregular rings had the greatest tendency to switch over the follow-up, whereas most cases of absent and regular rings remained stable over time. More specifically, we observed a wide range of possible changes in the SW-AF pattern: (1) absent to irregular; (2a) irregular to regular; (2b) irregular to absent; (3a) regular to irregular; and (3b) regular to absent.

Gathering all the information we collected, we propose that the modifications of the hyperAF ring could follow a chronological order. The starting point is the case of an intact EZ in the absence of the hyperAF ring. Subsequently, the EZ shrinks down to the point where an irregular ring develops, and from there one could face two different scenarios. The first possibility, which is the one that we observed more frequently, is that the hyperAF ring undergoes a "regularization" process; and the second option is to observe a gradual vanishing of the irregular ring, back to the absence of an observable hyperAF phenomenon. The current knowledge on the hyperAF ring leads to the conclusion that it corresponds to the area where the ELM directly lies upon the RPE, because it has been observed that outside its boundaries both the ELM itself and the EZ are completely disrupted, whereas on the other side these structures are both preserved.[8,11,24] Therefore, even if we did not specifically measure the ELM width for our study, we hypothesize that ring "regularization" seen on SW-AF images is the consequence of a faster constriction of the ELM, ultimately matching the EZ and leading to the formation of a regular hyperAF ring.

Finally, we observed that the regular hyperAF ring at the end of the follow-up could either have become an irregular ring, due to its partial disruption, or be completely faded, as already reported in literature.[6,10,25] Although this last case has been attributed to be the consequence of a complete disruption of the EZ, we believe that irregular ring disappearance may be caused by a different mechanism, because the EZ is still preserved. It is possible that, in this case, the ring gradually fades away because either a loss of ELM reflectivity or a diminished RPE-derived signal.

Our research has several shortcomings. First, because our retrospective study only featured baseline and last follow-up visits, it is possible that we have underestimated the proportion of patients undergoing a pattern switch on SW-AF images, potentially missing cases who experienced two consecutive changes in their autofluorescence pattern during this interval. Second, even though the inter-rater reliability for the assessment of the hyperAF ring was very good, some cases still required the judgment of an experienced grader. This challenge is expected to be addressed soon with the advancement of machine learning algorithms, which have the potential to provide a more impartial assessment of FAF images as technology progresses.[26,27] Additionally, our cohort mostly featured patients with autosomal recessive inheritance, including some syndromic cases, for whom we did not conduct separate disease progression analyses due to genotype heterogeneity, whereas patients with XL RP and AD RP were less represented. Moreover, no subanalyses focused on the genetic characterization was attempted owing to the limited number of patients enrolled in the study, which would have hampered a reliable assessment. Last, the quantification of the area covered by the hyperAF ring was not taken into account, because it is often hampered by the lack of definition of its boundaries in the case of irregular rings.

In conclusion, the presence of the hyperAF ring allows for an intuitive visualization of the preserved retina and provides useful indications on patients' BCVA, whereas its shape provides quick information regarding the expected constriction rate of those eye, as regular rings demonstrated

Investigative Ophthalmology & Visual Science

a substantial stability over time. On the other hand, eyes lacking an hyperAF ring but exhibit a measurable EZ should be closely monitored, as this particular FAF pattern could potentially indicate a faster rate of disease progression. Last, we provided a description of hyperAF ring changes over the course of the disease and postulated their chronological sequence. Future studies with a longer follow-up and a prospective design are warranted to confirm our hypotheses, which may aid clinicians in the interpretation of imaging findings modifications occurring in their patients.

Acknowledgments

Supported by Progetto di Ricerca Finalizzata Ministero della Salute NET2016.

Disclosure: **A. Antropoli**, None; **A. Arrigo**, None; **L. Bianco**, None; **E. Cavallari**, None; **F. Bandello**, Alcon, Fort Worth, TX, USA (C), Farmila-Thea, Clermont-Ferrand, France (C), Alimera Sciences, Alpharetta, GA, USA (C), Bausch & Lomb, Rochester, NY, USA (C), Allergan Inc., Irvine, CA, USA (C), Genentech, San Francisco, CA, USA (C), Hoffmann-La-Roche, Basel, Switzerland (C), Novagali Pharma, Evry, France (C), Novartis, Basel, Switzerland (C), Bayer Shering-Pharma, Berlin, Germany (C), Sanofi-Aventis, Paris, France (C), Thrombogenics, Heverlee, Belgium (C), Zeiss, Dublin, CA, USA (C), Pfizer, New York, NY, USA (C), Santen, Osaka, Japan (C), Sifi, Aci Sant'Antonio, Italy (C); **M. Battaglia Parodi**, None

References

1. Verbakel SK, van Huet RAC, Boon CJF, et al. Non-syndromic retinitis pigmentosa. *Prog Retin Eye Res*. 2018;66:157–186.
2. Delori FC, Dorey CK, Staurenghi G, Arend O, Goger DG, Weiter JJ. In vivo fluorescence of the ocular fundus exhibits retinal pigment epithelium lipofuscin characteristics. *Invest Ophthalmol Vis Sci*. 1995;36(3):718–729.
3. Iftikhar M, Usmani B, Sanyal A, et al. Progression of retinitis pigmentosa on multimodal imaging: the PREP-1 study. *Clin Exp Ophthalmol*. 2019;47(5):605–613.
4. Murakami T, Akimoto M, Ooto S, et al. Association between abnormal autofluorescence and photoreceptor disorganization in retinitis pigmentosa. *Am J Ophthalmol*. 2008;145(4):687–694.
5. Lenassi E, Troeger E, Wilke R, Hawlina M. Correlation between macular morphology and sensitivity in patients with retinitis pigmentosa and hyperautofluorescent ring. *Invest Ophthalmol Vis Sci*. 2012;53(1):47.
6. Robson AG, Lenassi E, Saihan Z, et al. Comparison of fundus autofluorescence with photopic and scotopic fine matrix mapping in patients with retinitis pigmentosa: 4- to 8-year follow-up. *Invest Ophthalmol Vis Sci*. 2012;53(10):6187.
7. Lima LH, Burke T, Greenstein VC, et al. Progressive constriction of the hyperautofluorescent ring in retinitis pigmentosa. *Am J Ophthalmol*. 2012;153(4):718–727.e2.
8. Lima LH, Cella W, Greenstein VC, et al. Structural assessment of hyperautofluorescent ring in patients with retinitis pigmentosa. *Retina*. 2009;29(7):1025–1031.
9. Lee J, Asano S, Inoue T, et al. Investigating the usefulness of fundus autofluorescence in retinitis pigmentosa. *Ophthalmol Retina*. 2018;2(10):1062–1070.
10. Robson AG, Tufail A, Fitzke F, et al. Serial imaging and structure-function correlates of high-density rings of fundus autofluorescence in retinitis pigmentosa. *Retina*. 2011;31(8):1670–1679.
11. Greenstein VC, Duncker T, Holopigian K, et al. Structural and functional changes associated with normal and abnormal fundus autofluorescence in patients with retinitis pigmentosa. *Retina*. 2012;32(2):349–357.
12. Jauregui R, Chan L, Oh JK, Cho A, Sparrow JR, Tsang SH. Disease asymmetry and hyperautofluorescent ring shape in retinitis pigmentosa patients. *Sci Rep*. 2020;10(1):3364.
13. Birch DG, Locke KG, Wen Y, Locke KI, Hoffman DR, Hood DC. Spectral-domain optical coherence tomography measures of outer segment layer progression in patients with X-linked retinitis pigmentosa. *JAMA Ophthalmol*. 2013;131(9):1143–1150.
14. Thiele S, Isselmann B, Pfau M, et al. Validation of an automated quantification of relative ellipsoid zone reflectivity on spectral domain-optical coherence tomography images. *Transl Vis Sci Technol*. 2020;9(11):17.
15. Komori S, Ueno S, Ito Y, et al. Steeper macular curvature in eyes with non-highly myopic retinitis pigmentosa. *Invest Ophthalmol Vis Sci*. 2019;60(8):3135–3141.
16. Kim YJ, Joe SG, Lee DH, Lee JY, Kim JG, Yoon YH. Correlations between spectral-domain OCT measurements and visual acuity in cystoid macular edema associated with retinitis pigmentosa. *Invest Ophthalmol Vis Sci*. 2013;54(2):1303–1309.
17. Sandberg MA, Brockhurst RJ, Gaudio AR, Berson EL. The association between visual acuity and central retinal thickness in retinitis pigmentosa. *Invest Ophthalmol Vis Sci*. 2005;46(9):3349–3354.
18. Aizawa S, Mitamura Y, Baba T, Hagiwara A, Ogata K, Yamamoto S. Correlation between visual function and photoreceptor inner/outer segment junction in patients with retinitis pigmentosa. *Eye (Lond)*. 2009;23(2):304–308.
19. Jauregui R, Takahashi VKL, Park KS, et al. Multimodal structural disease progression of retinitis pigmentosa according to mode of inheritance. *Sci Rep*. 2019;9(1):10712.
20. Hariri AH, Zhang HY, Ho A, et al. Quantification of ellipsoid zone changes in retinitis pigmentosa using en face spectral domain–optical coherence tomography. *JAMA Ophthalmol*. 2016;134(6):628.
21. Tee JJL, Kalitzeos A, Webster AR, Peto T, Michaelides M. Quantitative analysis of hyperautofluorescent rings to characterize the natural history and progression in RPGR-associated retinopathy. *Retina*. 2018;38(12):2401–2414.
22. Sujirakul T, Lin MK, Duong J, Wei Y, Lopez-Pintado S, Tsang SH. Multimodal imaging of central retinal disease progression in a 2-year mean follow-up of retinitis pigmentosa. *Am J Ophthalmol*. 2015;160(4):786–798.e4.
23. Cabral T, Sengillo JD, Duong JK, et al. Retrospective analysis of structural disease progression in retinitis pigmentosa utilizing multimodal imaging. *Sci Rep*. 2017;7(1):10347.
24. Hood DC, Lazow MA, Locke KG, Greenstein VC, Birch DG. The transition zone between healthy and diseased retina in patients with retinitis pigmentosa. *Invest Ophthalmol Vis Sci*. 2011;52(1):101–108.
25. Wakabayashi T, Sawa M, Gomi F, Tsujikawa M. Correlation of fundus autofluorescence with photoreceptor morphology and functional changes in eyes with retinitis pigmentosa. *Acta Ophthalmol*. 2009;88(5):e177–e183.
26. Nagasato D, Sogawa T, Tanabe M, et al. Estimation of visual function using deep learning from ultra-widefield fundus images of eyes with retinitis pigmentosa. *JAMA Ophthalmol*. 2023;141(4):305–313.
27. Charng J, Viedma I, Alonso-Caneiro D, Mackey DA, Chen FK. A wavelength-agnostic, deep learning algorithm segmenting the hyperautofluorescent ring in retinitis pigmentosa. *Invest Ophthalmol Vis Sci*. 2022;63(7):2073–F0062.

Investigative Ophthalmology & Visual Science